Temperature-Dependent Excitonic Decay and Multiple States in Single-Wall Carbon Nanotubes

Wyatt K. Metzger,[*,†] **Timothy J. McDonald,**[†,‡] **Chaiwat Engtrakul,**[†] **Jeffrey L. Blackburn,**[†] **Gregory D. Scholes,**[§] **Garry Rumbles,**[†] **and Michael J. Heben**[†]

National Renewable Energy Laboratory, 1617 Cole Boulevard, Golden, Colorado 80401-3393, Department of Applied Physics, Columbia University, New York, New York 10027 and Centre for Quantum Information and Quantum Control and Institute for Optical Sciences, Lash-Miller Chemical Laboratories, 80 St. George Street, University of Toronto, Toronto, Ontario, Canada M5S 3H6

We have performed steady-state photoluminescence, time-correlated single photon counting, and Raman spectroscopy measurements on single-wall carbon nanotubes from 4 to 293 K. We observe novel photoluminescence spectra that cannot be attributed to vibronic transitions and verify the existence and energy levels of weakly emissive excitonic states. By combining photoluminescence intensity and lifetime data, we determine how nonradiative and radiative excitonic decay rates change as a function of temperature and contrast this with theoretical predictions. The results suggest that recombination kinetics are influenced by multiple excitonic states, including a dark lower state.

Introduction

The discovery of single-wall carbon nanotubes (SWNTs) in 1993[1,2] sparked the imagination of many researchers who saw these nanocylindrical structures as appealing candidates for ballistic electrical transport and novel electro-optical devices. Many years later, scientists are realizing some of the applications initially envisioned. But to understand both the full potential and practical limitations of nanotubes in devices, especially with respect to their possible application in solar energy conversion,[3,4] requires a better scientific understanding of electronic structure, excitonic decay, and transport properties. Recently, the one-electron band model of SWNT transitions has been replaced with a model in which the absorption of light produces excitons.[5,6] Consequently, many electro-optical experiments have been interpreted by assuming that light emission and transport occur within a single excitonic band after thermalization. We present experimental evidence that there are actually multiple excitonic states, each with different recombination properties, which affect excitonic kinetics in SWNTs.

As-produced SWNTs contain an inhomogeneous, bundled mixture of nanotubes with metallic and semiconducting character in which the metallic SWNTs quench luminescence from semiconducting nanotubes. As a result, it was not until 2002 when tube bundling was sufficiently reduced by new processing techniques that band gap photoluminescence (PL) was first observed.[7,8] Since then, steady-state[7–14] and time-resolved[15–20] PL studies have shown that thermalization occurs in less than 1 ps, and although long-lived components have been observed the majority of excitons subsequently decay with lifetimes in the range of 5–200 ps.[15–25] Because experimental estimates of the radiative quantum efficiency typically range from 10^{-3} to $10^{-4,15–18}$ researchers believe the primary decay process is nonradiative. Various studies indicate that extrinsic properties

influence the recombination rate,[17–19,21,25,26] as demonstrated by one recent study that measures lifetimes that vary from 20 to 180 ps for individual tubes of the same (*n*, *m*) species.[17] The intrinsic radiative lifetime is determined experimentally by measuring the nonradiative lifetime and estimating the radiative quantum efficiency. Values for the radiative lifetime range from 10 ns to 10 μs.[15–18]

Very little is experimentally known about the nonradiative decay mechanisms and the related excitonic states in SWNTs. Recent theoretical calculations indicate that multiple excitonic states may affect recombination kinetics. Perebeinos et al.[26] and Spataru et al.[27] predict that the lowest spin singlet exciton ($_0B_0^-$) for any zigzag or chiral semiconducting SWNT is optically forbidden, the second-lowest exciton ($_0A_0^-$) is optically allowed, and the third-lowest excitons ($_0E_6^-$) are optically forbidden (the ordering may vary at nonzero momentum). Zhao and Mazumdar[28] predict four excitonic states: the highest is strongly coupled to the radiation field, the lowest is optically forbidden, and the two intermediate states are weakly allowed. These excitons are predicted to be separated from one another by several meV to tens of meV, and symmetry breaking by defects or ambient conditions may allow scattering of optically excited states into the lowest energy dark state or cause the lowest dark state to become weakly radiative.

The possibility of a multiplet of coupled excitonic bands has strong implications for the temperature dependence of the effective radiative lifetime. The radiative recombination rate is predicted to increase with decreasing temperature for bright excitons that do not couple to other states. However, if excitons scatter efficiently into the lowest dark state, there will be insufficient thermal energy for re-emission from this state at low temperatures, and the effective radiative recombination rate will fall precipitously with temperature.[26,27]

In this article, we first discuss PL excitation (PLE) spectral features that may be caused by multiple excitonic states. Then, we analyze time-resolved photoluminescence data to examine how nonradiative recombination varies as a function of tem-

---

* Corresponding author. E-mail: wyatt_metzger@nrel.gov.
† National Renewable Energy Laboratory.
‡ Columbia University.
§ Lash-Miller Chemical Laboratories.
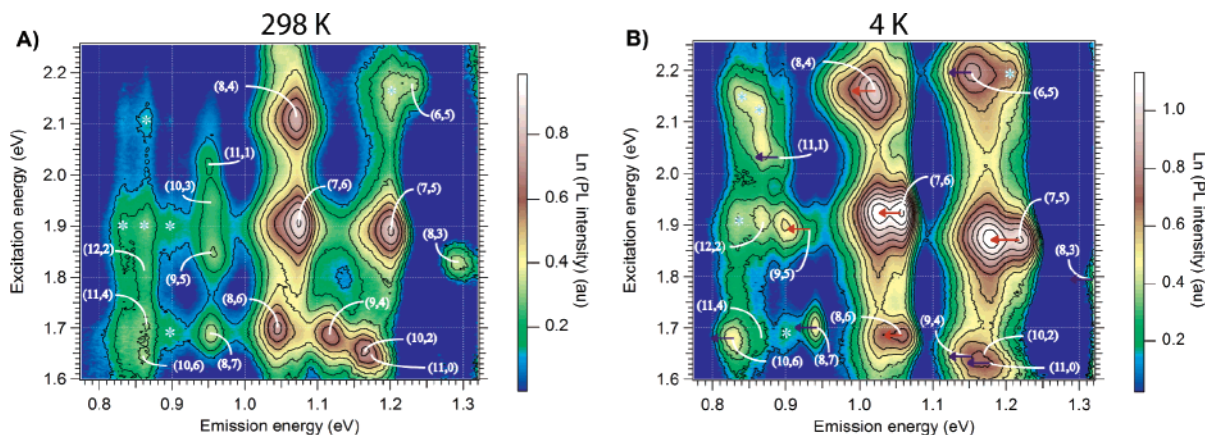
Figure 1. PLE spectra from SWNTs dispersed in SDS and *AQ55* polymer at (a) RT and (b) 4 K. The red arrows point to the location of a second lower energy peak, *W*, and the blue arrows point to a region of the plot where the *W* peak is absent. The teal asterisks refer to peaks assigned to phonon-assisted transitions.

perature. Finally, the time-resolved data is combined with PL intensity data to estimate how radiative recombination varies with temperature, which affords a comparison with the recombination kinetics predicted to occur in the presence of multiple excitonic states.

Experiment

To obtain a sample with well-behaved optical properties across the full temperature range of interest, we isolated HiPco (Carbon Nanotechnologies) SWNTs in an aqueous surfactant, added *AQ55* polymer (Eastman Chemical Company), stirred, and lyophilized to form a dry powder.[29] The resulting polymer/SWNT powders remain a single phase over the temperature range investigated.

PLE spectra were obtained with a modified Thermo-Electron FT960 Raman system,[30] which contains a Ge detector operating at 77 K that responds to wavelengths between 900 and 1700 nm. The excitation source was a 250 W tungsten halogen bulb coupled to a single-grating monochromator, which produces monochromatic light between 400 and 1100 nm with a peak power at 700 nm of 1.7 mW. All spectra were corrected for intensity variations in the lamp spectrum, as well as for the response of the system and detector.

PL decay curves were measured by time-correlated single-photon counting.[31] Photoexcitation at the E_2 wavelength was provided by an optical parametric amplifier pumped by the output of a titanium−sapphire laser system with a regenerative amplifier. The final laser output consisted of a 250 kHz pulse train with a pulse width of several hundred femtoseconds and a beam focused to several hundred microns in diameter. The measurements were performed with ∼4 nJ per pulse except in the case of (9,5) tubes, which required 40 nJ per pulse. The PL was passed through long-pass filters and a spectrometer tuned to the E_1 wavelength and detected by a cooled (80 K), infrared-sensitive photomultiplier tube. Instrument response functions (IRFs) were measured using scattered light from the sample. PL decay curves were analyzed by nonlinear least-squares iterative reconvolution of a model exponential-decay function with the measured instrument-response functions.[32] This technique removes the contribution of the IRF to the measured decay, resulting in a temporal resolution of about 10% of the instrument-response function width, which is about 30 ps in these data.

Raman spectra were obtained with a Spex 270M monochromator using 1.96 eV (633 nm) laser excitation. The laser power was kept at 4.0 mW to avoid sample heating and the slit width

was 0.1 mm, allowing for a resolution of 2−4 cm^{-1} across the measured spectrum. The powder sample was placed onto the cold finger of an MMR Joule-Thomson refrigeration system (Model K2001) using Apiezon thermal grease and cooled with high-pressure (1800-psi) nitrogen stream (4 cf/h) with a temperature resolution of ±2 K.

Results and Discussion

(i) PLE and Raman Spectra. Figure 1 shows PLE spectra from SWNTs in the *AQ55* polymer matrix at room temperature and 4 K. PL from specific nanotubes create maxima in the contour plot when the excitation energy (ordinate) is resonant with the second-lowest energy transition, E_2, and emission (abscissa) is detected at the energy of the lowest energy transition, E_1. Each maximum is assigned by comparing with tight-binding theory and noting trends in structurally related nanotubes;[8] this method has been confirmed by density functional theory, which considers the effects of multiple carriers and excitons.[33]

A comparison of the room temperature (RT) and 4 K PLE data (Figure 1) shows that that the peak emission and excitation energies associated with individual tubes change significantly as a function of temperature. The energy shifts are a consequence of two effects: (i) external strain imposed by the encapsulating polymer matrix, which shifts the band gap to either higher or lower energy depending on the nanotube's (n, m) index, and (ii) an intrinsic band gap shift to higher energy at lower temperatures. An earlier article from our group quantifies the influence of each of these two effects as a function of temperature for more than 10 nanotubes in the same *AQ55* matrix.[29] Applying the same methods here, we find that the intrinsic band gap shifts 12−15 meV between 4 and 293 K for each nanotube. The remainder of the wavelength shift is caused by strain, which causes PL from nanotubes with $(n − m)\mathrm{mod}3 = 2$ to emit at higher energy with decreasing temperatures, and PL from nanotubes with $(n − m)\mathrm{mod}3 = 1$ to emit at lower energies.[34,35]

In addition to the previously observed shifts in the peak emission and excitation energies, a low-energy emission peak, labeled *W*, becomes prominent for certain tubes at low temperatures (Figure 1). For example, Figure 2 is a slice through the contour data that shows the emission from the (7,6) nanotube species. As the temperature is reduced below 100 K, a fully resolved second emission becomes obvious. This peak also appears for the (7,5), (8,4), (8,6) and (9,5) nanotubes and maximizes at precisely the same excitation energy as the

Excitonic Decay and Multiple States in SWCNs

J. Phys. Chem. C, Vol. 111, No. 9, 2007 **3603**
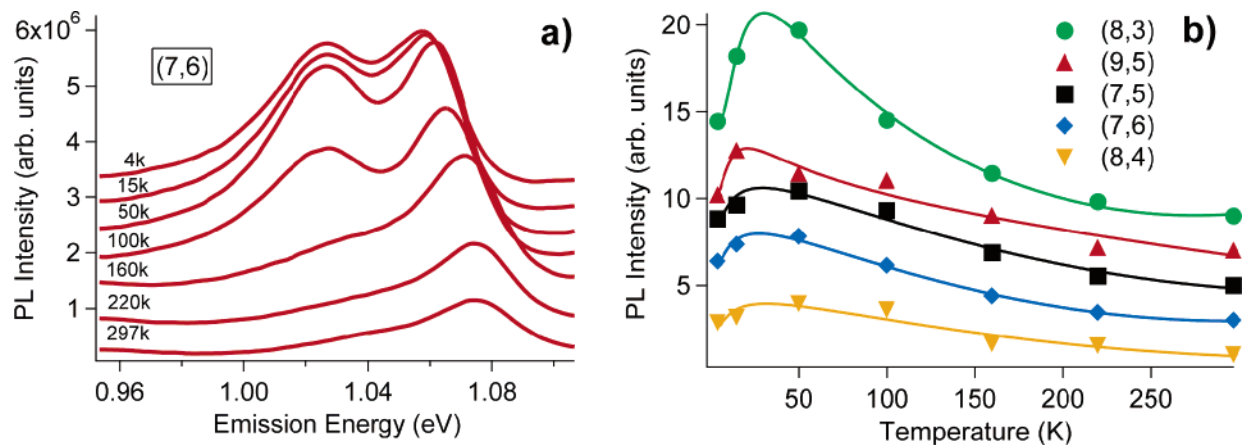
Figure 2. (a) PL emission spectra at various temperatures when the excitation wavelength is resonant with the second-lowest energy transition of the (7,6) nanotube species. (b) Integrated PL intensity at different temperatures. Vertical offsets have been added to the data. The lines in panel b are only to guide the eye.

E_2 transition at different temperatures. This, combined with an examination of the E_1 and E_2 values observed in PLE contour plots taken over seven different temperatures (not shown), indicates that the W peak is not generated by tubes of different chirality. By fitting the peaks of the various features shown in Figure 1 and extrapolating their PL contribution to the position of the W peaks, we can conclude also that there is not enough off resonance emission from neighboring nanotubes to create the W peaks.

Figure 2b illustrates how the integrated PL intensity varies with temperature when contributions from both the E_1 peak and the W peak are included. The intensity for each tube is normalized to one at room temperature and offset for presentation. Below 100 K, the W and E_1 peaks are fully resolved, but their relative intensities do not change significantly as the temperature is reduced to 4K (Figure 2a). However, both peaks drop in intensity as the temperature is reduced from 50 to 4 K. These data suggest that in addition to the E_1 state, there is a dark state that has an energy level below both the W and E_1 transitions, as predicted theoretically.

To explain the data, one can consider two possible models (Figure 3). In model A, the W peak is attributed to a phonon-assisted radiative transition, and the overall decrease in the PL intensity below 50 K is attributed to a low-energy dark state. Phonon emission or absorption can increase the number of possible initial and final states that conserve energy and momentum during a radiative transition. This may enhance the W transition probability relative to the E_1 transition at lower
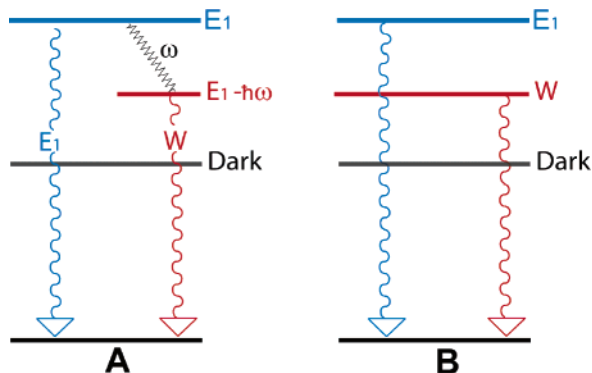
temperatures, and thereby describe the PL intensity changes seen in Figure 2a. One can test if the W peak is related to a particular phonon or vibronic mode by examining the PL spectra in more detail. The separation between the E_1 and W peaks at 4 K was estimated by fitting the data with Voigt functions and is shown in Figure 4a. The W peak is red-shifted relative to the E_1 transition by 20−50 meV, and the energy difference scales inversely with tube diameter. The only vibronic mode with a resonant energy of this magnitude that scales similarly with tube diameter is the radial breathing mode (RBM).

To characterize how the RBM is affected by temperature and strain, we measured Raman spectra for the (7,6) and the (7,5) tubes between 80 and 293 K on the same *AQ55* polymer matrix used in the PL studies. The W peaks are not easily resolved above 100 K; however, comparisons between Raman and PL measurements can be made at intermediate temperatures. The Raman frequency and intensity for the RBM are nearly constant between 80 and 300 K despite strain. In contrast, the separation between the E_1 and W peaks shifts with temperature. In addition, Figure 4b shows that around 80 K, the energy separation between E_1 and W does not match the RBM energy. Thus, it is unlikely that the W peak is a phonon-assisted transition involving the RBM. Because we do not know of any other vibronic transition that could describe the experimental data, an alternative explanation is needed.

A different explanation, consistent with model B, is that the W peak is due to emission from one of the weakly allowed intermediate states predicted by Zhao and Mazumbdar.[28] Alternatively, the W peak could be the manifestation of a normally dark state made weakly radiative through symmetry breaking by impurities, the ambient, strain, or other experimental conditions. This explanation readily describes the data in Figure 4a because the energy separation between these excitonic states is predicted to depend on tube diameter,[26] but these data do not eliminate the possibility that the weakly emissive state in model B is created by defects. Model B also gives a natural explanation for the intensity shifts in Figures 1 and 2. As the temperature is reduced from RT, excitons populate the lower-energy states, thereby increasing the intensity of the W peak.

In our data, the W peak appears for many different nanotube species but not all of them. The inconsistent appearance of this peak is more easily described by a defect state or an excitonic state that requires symmetry breaking to become radiative than by model A. One might expect that if the source of the W emission were an intrinsic excitonic band, it would appear

Figure 3. Energy diagrams illustrating models A and B. In model A, the W peak is caused by a radiative transition assisted by a phonon or vibronic mode with energy $\hbar\omega$. In model B, the W peak emerges from a distinct electronic state.
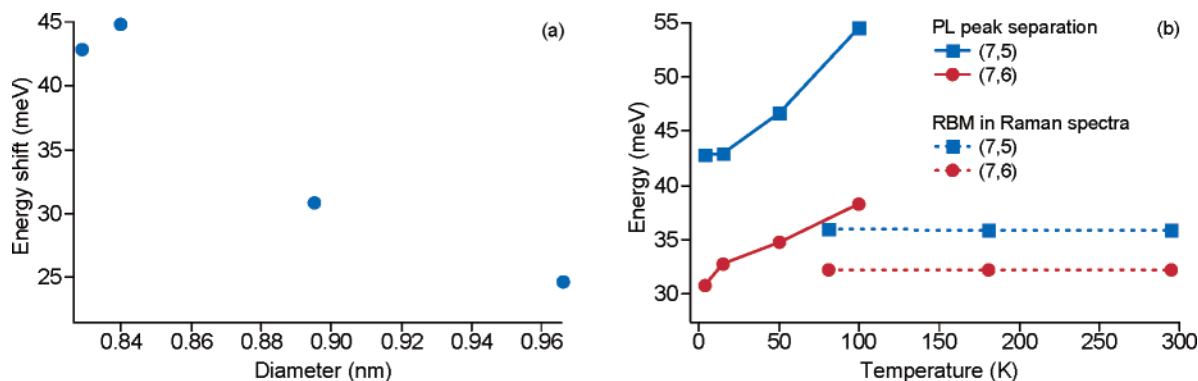
Figure 4. (a) The energy separation at 4 K between the E_1 and W peaks as a function of tube diameter for four nanotube species. (b) A comparison of the PL peak separation and the RBM energy determined by Raman spectra at different temperatures.

consistently in other low-temperature PL studies. However, the radiative efficiency and scattering from the E_1 state into these weakly emissive bands is predicted to depend sensitively on the sample and its surrounding environment. The PL excitation and detection setup is also important. For example, in an earlier work,[29] W peaks for the (7,5) and (7,6) peaks were observed when exciting near resonance, 650 nm. However at 590 nm, these same peaks had less intensity and were obscured by overlapping PL emission from nanotubes that are brighter at this excitation wavelength. Sample preparation and PL configurations have varied appreciably among the small number of low-temperature SWNT studies. Yet, emission features similar to the W peaks do appear in most other low-temperature experiments[17,29,36,37] though not always.[38] Here, we cannot distinguish if the W peak is a defect state or an intrinsic excitonic band, but it does appear to be a distinct excitonic state that influences recombination kinetics.

(ii) Time-Correlated Single Photon Counting Data. Next, we examine the nonradiative recombination rates associated with the excitonic transitions observed in the PL spectra. At the injection levels used in the time-resolved PL (TRPL) experiments, the PL intensity is proportional to the exciton population. As was stated earlier, quantum efficiency measurements indicate that only between 10^{-3} and 10^{-4} of all excitons decay radiatively in SWNTs,[15-18] so time-resolved PL primarily tracks nonradiative decay. Figure 5a shows representative decay data as well as the system response. The decays required a biexponential function to be fit, but the second exponent has a yield below 10%. The lifetimes of the dominant decay component are shown in Figure 5b for different tube species as a function of temperature. As the temperature decrease from RT to 4 K, the lifetimes increase from 50 to 150%.

This relatively small change in lifetime is inconsistent with recombination processes involving a scattering matrix that is sensitive to temperature. Hagen et al.[17] modeled SWNT recombination kinetics with rate equations that involve an activation energy, E_A, and phonons with an average frequency, ω_m. The formulas were derived generically for nonradiative transitions in large molecules and not specifically for carbon nanotubes.[39] Nonetheless, the theory is qualitatively appealing. During nonradiative transitions, energy and momentum are imparted to the nanotube in the form of phonons. The lifetime varies significantly with temperature only if the average phonon energy is less than ~60 meV. Again, this suggests the RBM phonon. Because the RBM is diameter dependent, the nonradiative lifetime also should be diameter dependent. Figure 6 shows a clear dependence of lifetime on tube diameter at RT, and we observed a similar trend for over 15 tube species in solution in a separate study.[40] The theory also can describe the relatively small increase in the nonradiative lifetime from 4 to 293 K. However, the model fails quantitatively for our data. The magnitude of the lifetime change between 4 and 293 K can be fit if the E_A is less than 40 meV, but the diameter dependence of the lifetimes at RT can only be fit with E_A greater than 150 meV. In addition, the theory indicates that the lifetime should be nearly constant between 4 and 50 K, but this is generally not observed. Finally, the strong coupling limit[39] on which the theory is predicated is not in agreement with measured values of the Stokes shift on carbon nanotubes.[15] Perhaps a similar theory developed directly for SWNTs could reconcile these differences. The diameter dependence of nonradiative recombination could stem from how excitonic wavefunctions vary in tubes of different diameter.

TRPL measurements were also performed at the emission energies corresponding to the W peaks for the (7,5) and (7,6) tubes. Figure 7 indicates the data taken at 4 K for the (7,5) nanotube, which is nearly identical to the data for the (7,6) tube. There is a significant difference between the PL decay
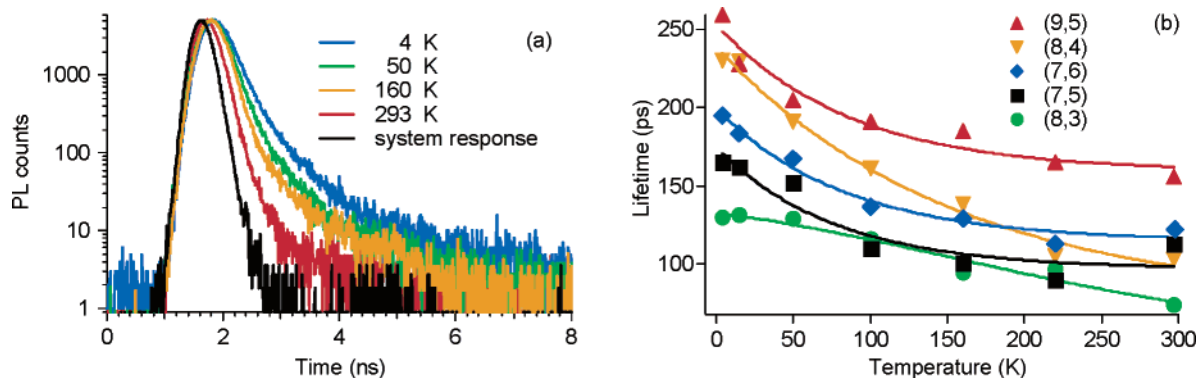
Figure 5. (a) Luminescence decay profiles from the (8,4) nanotube species. (b) PL lifetimes at different temperatures. The lines are to guide the eye.
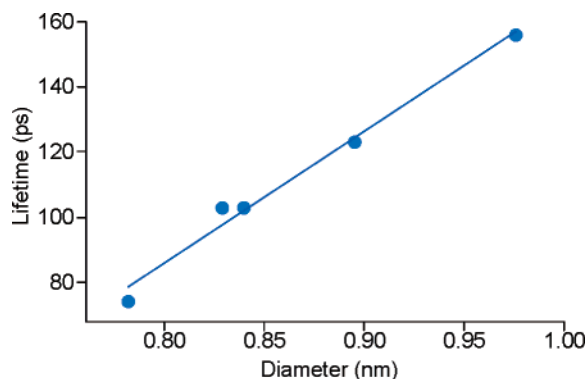
Figure 6. Lifetime vs tube diameter at RT. The line is a linear fit to the data given by lifetime (ps) = 404*diameter (nm) − 238.
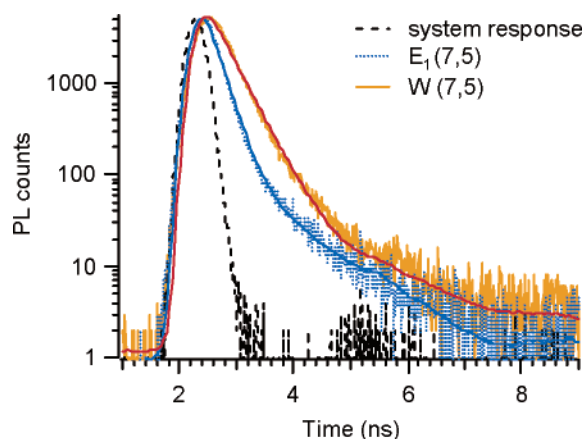
Figure 7. PL decay data for the (7,5) nanotube at 4 K. The lines through the data are reconvoluted biexponential fits.

of the E_1 and W peaks. This is further evidence that the W peak is generated by a distinct excitonic state, rather than a phonon-assisted transition. The initial PL decay time shown for the W peak is 350 ps when fitting with a biexponential decay function. Incorporating a single-exponential rise time of 190 ps, commensurate with the initial decay time of the E_1 emission, and modifying the initial decay time of the W peak to 240 ps improves the curve fitting. However, the effects are too subtle to unequivocally determine a rise time in the time-resolved PL data from the W emission.

(iii) The Effective Radiative Recombination Rate. For the E_1 state, the effective radiative recombination rate, w_r is estimated by dividing the integrated PL intensity of the E_1 peak (separated out from the W peak by careful fitting with Voigt functions) by the nonradiative lifetime. Similar to the PL intensity at temperatures greater than 50 K w_r generally decreases with increasing temperature. Theoretically, this is

expected to occur because the radiative recombination rate decreases with exciton momentum, which on average increases with temperature.[26,27] Calculations by Perebeinos et al.[26] predict that the temperature dependence of w_r will scale as $T^{-3/2}$ at higher temperatures and continue to increase at low temperatures if there is no coupling between the singlet exciton band with odd parity (the E_1 transition is attributed to this excitonic state) and other excitonic bands. Figure 8a shows this case, which we term "single band kinetics", along with the experimental data for the (7,6) tube. Although there is good agreement at the higher temperatures, the data and theory diverge strongly as the temperature is reduced below ∼200 K. In contrast, if the (7,6) tube data is plotted along with expectations for w_r based on scattering between multiple excitonic states ("multiple band kinetics", Figure 8b), we see a relatively good agreement of the functional form across the entire temperature range. The other nanotubes that were measured show the same behavior. The functional form emerges because at lower temperatures the lower-energy dark state is populated and the apparent emission from the E_1 state decreases, thereby reducing w_r. The theoretical curve shown in Figure 8b is determined under the assumption that the excitons are partitioned in the multiple states according to the Boltzman distribution. Hence, at low temperatures nearly every exciton is in the dark exciton state, and the effective radiative recombination falls to zero. In experiment, excitons generated in the emissive states may recombine nonradiatively and radiatively prior to scattering into the dark exciton state. The kinetics in our experiment imply that at low temperatures there is still reasonable radiative efficiency, and hence some excitons are recombining radiatively prior to scattering into lower states. For example, the PL spectral and intensity changes shown here can be quantitatively reproduced in computer simulations by using a three-state model with a strongly radiative (E_1) top state, a weakly emissive intermediate state (W), a dark bottom state, and experimental parameters in general agreement with the PLE and time-resolved PL data, if the scattering time into the lower states is assumed to be on the order of the PL decay times.[41]

Conclusion

We observe novel PL spectra that cannot be attributed to vibronic transitions and verify the existence and energy levels of weakly emissive excitonic states. Low-temperature TRPL measurements indicate that the dominant nonradiative lifetime changes only by about a factor of 2 between 4 and 293 K. The effective radiative recombination rate increases as the temperature is lowered from RT to intermediate temperatures, around 50 K, while at lower temperatures the rate decreases. Together, these data suggest that recombination and transport

Figure 8. Normalized curves indicating how w_r changes as a function of temperature for the (7,6) tube and theoretically[26] for zigzag tubes with a diameter of 1.0 nm in a medium having a dielectric constant, ϵ, equal to 2. (a) Single band kinetics refers to theoretical prediction when only the singlet band of odd parity affects kinetics. (b) Scattering between singlet bands of different parity allows for multiple band kinetics. The presence of a dark lower state causes w_r to decrease below ∼50 K.

Metzger et al.

are influenced by multiple exciton states, including a dark lower state.

Although optical pumping will generally populate the E_1 state, excitonic diffusion lengths and transport properties can be governed by the properties of other states. If these states are intrinsic excitonic bands, this implies that many lifetime measurements may not be measuring the only decay time that is relevant for electro-optical nanotube devices. The long lifetimes of the low-energy peaks measured here suggests that there could be other bands that may have different excitonic decay and transport properties that are potentially useful.

Note Added after ASAP Publication. This article was published ASAP on February 3, 2007. A text change has been made in the fourth paragraph of the Results and Discussion Section. The corrected version was published on February 8, 2007.

References and Notes

(1) Bethune, D. S.; Kiang, C. H.; Devries, M. S.; Gorman, G.; Savoy, R.; Vazquez, J.; Beyers, R. *Nature* **1993**, *363,* 605.

(2) Iijima, S.; Ichihashi, T. *Nature* **1993**, *363*, 603.

(3) Stewart, D. A.; Leonard, F. *Nano Lett.* **2005**, *5*, 219.

(4) Barazzouk, S.; Hotchandani, S.; Vinodgopal, K.; Kamat, P. V. *J. Phys. Chem. B* **2004**, *108*, 17015.

(5) Ando, T. *J. Phys. Soc. Jpn.* **1997**, *66*, 1066.

(6) Wang, F.; Dukovic, G.; Brus, L. E.; Heinz, T. F. *Science* **2005**, *308*, 838.

(7) Bachilo, S. M.; Strano, M. S.; Kittrell, C.; Hauge, R. H.; Smalley, R. E.; Weisman, R. B. *Science* **2002**, *298*, 2361.

(8) O'Connell, M. J.; Bachilo, S. M.; Huffman, C. B.; Moore, V. C.; Strano, M. S.; Haroz, E. H.; Rialon, K. L.; Boul, P. J.; Noon, W. H.; Kittrell, C.; Ma, J. P.; Hauge, R. H.; Weisman, R. B.; Smalley, R. B. *Science* **2002**, *297*, 593.

(9) Hartschuh, A.; Pedrosa, H. N.; Novotny, L.; Krauss, T. D. *Science* **2003**, *301*, 1354.

(10) Weisman, R. B.; Bachilo, S. M. *Nano Lett.* **2003**, *3*, 1235.

(11) Lefebvre, J.; Fraser, J. M.; Homma, Y.; Finnie, P. *Appl. Phys. A* **2004**, *8*, 1107.

(12) Weisman, R. B.; Bachilo, S. M.; Tsyboulski, D. *Appl. Phys. A* **2004**, *78*, 1111.

(13) Lefebvre, J.; Fraser, J. M.; Finnie, P.; Homma, Y. *Phys. Rev. B* **2004**, *69,* 075403.

(14) Lebedkin, S.; Arnold, K.; Hennrich, F.; Krupke, R.; Renker, B.; Kappes, M. M. *New J. Phys.* **2003**, *5*, 140.

(15) Jones, M.; Engtrakul, C.; Metzger, W. K.; Ellingson, R. J.; Nozik, A. J.; Heben, M. J.; Rumbles, G. *Phys. Rev. B* **2005**, *71*, 115246.

(16) Hagen, A.; Moos, G.; Talalaev, V.; Hertel, T. *Appl. Phys. A* **2004**, *78*, 1137.

(17) Hagen, A.; Steiner, M.; Raschke, M. B.; Lienau, C.; Hertel, T.; Qian, H. H.; Meixner, A. J.; Hartschuh, A. *Phys. Rev. Lett.* **2005**, *95*, 197401.

(18) Wang, F.; Dukovic, G.; Brus, L. E.; Heinz, T. F. *Phys. Rev. Lett.* **2004**, *92*, 177401.

(19) Ma, Y. Z.; Stenger, J.; Zimmermann, J.; Bachilo, S. M.; Smalley, R. E.; Weisman, R. B.; Fleming, G. R. *J. Chem. Phys.* **2004**, *120*, 3368.

(20) Hertel, T.; Hagen, A.; Talalaev, V.; Arnold, K.; Hennrich, F.; Kappes, M.; Rosenthal, S.; McBride, J.; Ulbricht, J.; Flahaut, E. *Nano Lett.* **2005**, *5*, 511.

(21) Reich, S.; Dworzak, M.; Hoffman, A.; Thomsen, C.; Strano, M. S. *Phys. Rev. B* **2005**, *71*, 033402.

(22) Korovyanko, O. J.; Sheng, C. X.; Vardeny, Z. V.; Dalton, A. B.; Baughman, R. H. *Phys. Rev. Lett.* **2004**, *92*, 017403.

(23) Lauret, J. S.; Voisin, C.; Cassabois, G.; Delalande, C.; Roussignol, P.; Jost, O.; Capes, L. *Phys. Rev. Lett.* **2003**, *90*, 057404.

(24) Huang L.; Pedrosa, H. N.*;* Krauss, T. D. *Phys. Rev. Lett.* **2004**, *93*, 017403.

(25) Ostojic, G. N.; Zaric, S.; Kono, J.; Strano, M. S.; Moore, V. C.; Hauge, R. H.; Smalley, R. E. *Phys. Rev. Lett.* **2004**, *92*, 117402.

(26) Perebeinos, V.; Tersoff, J.; Avouris, P. *Nano Lett.* **2005**, *5*, 2495.

(27) Spataru, C. D.; Ismail-Beigi, S.; Capaz, R. B.; Louie, S. G. *Phys. Rev. Lett.* **2005**, *95*, 247402.

(28) Zhao, H.; Mazumdar, S. *Phys. Rev. Lett.* **2004**, *93*, 157402.

(29) Karaiskaj, D.; Engtrakul, C.; McDonald, T.; Heben, M. J.; Mascarenhas, A. *Phys. Rev. Lett.* **2004**, *96*, 106805.

(30) McDonald, T. J.; Jones, M.; Engtrakul, C.; Ellingson, R. J.; Rumbles, G.; Heben, M. J. *Rev. Sci. Instrum.* **2006**, *77*, 053104.

(31) O'Connor, D. V.; Phillips, D. *Time-Correlated Single Photon Counting*; Academic Press: San Francisco, CA, 1984.

(32) Grinvald, A.; Steinberg, I. Z. *Anal. Biochem.* **1974**, *59*, 583.

(33) Barone, V.; Peralta, J. E.; Wert, M.; Heyd, J.; Scuseria, G. E. *Nano Lett.* **2005**, *5*, 1621.

(34) Yang, L.; Anantram, M. P.; Han, J.; Lu, J. P. *Phys. Rev. B* **1999**, *60*, 13874.

(35) Yang, L.; Han, J. *Phys. Rev. Lett.* **2000**, *85*, 154.

(36) Lefebvre, J.; Finnie, P.; Homma, Y. *Phys. Rev. B* **2004**, *70,* 045419.

(37) Arnold, K.; Lebedkin, S.; Kiowski, O.; Hennrich, F.; Kappes, M. *Nano Lett.* **2004**, *4*, 2349.

(38) Li, L.; Nicholas, R. J.; Deacon, R. S.; Shields, P. A.; *Physical Review Letters* **2004**, *93*, 156104.

(39) Englman, R.; Jortner, J. *Mol. Physics* **1970**, *18*, 145.

(40) Jones, M.; Metzger, W. K.; McDonald, T.; Engtrakul, C.; Ellingson, R. J.; Rumbles, G.; Heben, M. J. *Nano Lett.* [Online early access]. DOI: 10.1021/nl0622808. Published Online: Jan 23, 2007. http://pubs.acs.org/cgi-bin/asap.cgi/nalefd/asap/html/nl0622808.html.

(41) Scholes, G. D.; McDonald, T.; Metzger, W. K.; Engtrakul, C.; Rumbles, G.; Heben, M. J. *J. Phys. Chem.*, submitted.